Biological Patterns

Thursday, Sept. 3: 11:00 – 13:00

Session 1: Audi Max

Contents

1

Computation of the Response Functions of spiral waves in active media

I.V. Biktasheva[1], D. Barkley[2], V.N. Biktashev[3], G.V. Bordyugov[1,4], and A.J. Foulkes[1]

[1] Dept of Computer Sci, University of Liverpool, Liverpool L69 3BX, UK
[2] Mathematics Institute, University of Warwick, Coventry CV4 7AL, UK
[3] Dept of Appl Maths, University of Liverpool, Liverpool L69 7ZL, UK
[4] present: Dept of Phys & Astronomy, University of Potsdam, 14476 Potsdam, Germany

Autowave vortices are types of self-organization observed in dissipative media of physical, chemical, and biological nature, where wave propagation is supported by a source of energy stored in the medium.

If slightly perturbed, spiral waves may drift, *i.e.* change rotational phase and/or center location. The response functions (RFs) of a spiral wave are the eigenfunctions of the adjoint linearized operator corresponding to the critical eigenvalues $\lambda = 0, \pm i\omega$. The RFs describe the spiral's sensitivity to small perturbations in the way that a spiral is insensitive to small perturbations where its RFs are close to zero. The velocity of a spiral's drift is proportional to the convolution of RFs with the perturbation.

Thus, an explicit knowledge of the Response Functions makes possible a quantitative prediction of the drift in numerous applications, *e.g.* control of re-entry in the heart. Biktasheva *et al.* [2] computed the RFs in the complex Ginzburg-Landau equation (CGLE) using an additional symmetry present in the CGLE, which permitted the reduction of the 2D problem to the computation of 1D components. It was shown that in the CGLE the RFs are localized at the tip of the spiral for all stable spiral wave solutions and qualitatively change at crossing the charachteristic lines in the model parameter plane. Subsequently, the computed RFs were successfully used for quantitative prediction of the spiral's resonant drift and drift due to media inhomogeneity [3].

For cardiac applications, dynamics of spiral waves in *excitable* media is more important than in *oscillatory* media such as the CGLE, as most cardiac tissues are excitable. These models do not allow reduction to 1D, making quantitatively accurate computation of the response functions more challenging. So far, the response functions have been computed in the Barkley [4, 5] and FitzHugh-Nagumo [6] models of excitable media. Hamm [4] and Biktasheva *et al.* [6] calculated RFs on Cartesian grids, but the accuracy was not sufficient for quantitative prediction of drift. Hakim and Henry [5] took the advantage of a polar grid and Barkley model to compute the spiral wave solution with an accuracy of 10^{-8} and RFs with accuracy 10^{-6} (both in the sense of l_2-norm of the residue of the discretized equations) leading to quantitative prediction of drift velocities with about 4% accuracy. Encouraging as these results are, there is a need for a more computationally efficient, accurate and robust method to compute the response functions of spiral waves in a variety of excitable media with required accuracy.

Here [1] we present a method which is superior to previous methods used to compute response functions, and demonstrate that it works for stationary rotating spirals in FitzHugh-Nagumo system. We also demonstrate convergence of the method with respect to the computational parameters, *i.e.* discretization steps and size of the medium.

The computed response functions are localized in the vicinity of the spiral wave tip and exponentially decay with distance from it. The eigenvectors of the linearized operator, *i.e.* Goldstone modes and of its adjoint, *i.e.* the response functions have been computed using the same technique, so the qualitatively different behavior of these solutions at large ρ is not a numerical artefact, as it was not in any way assumed in the numerical method.

Although the method has been used here to compute the response functions in the FitzHugh-Nagumo model, none of the details of the method depends on any specifics of the particular reaction kinetics and should be widely applicable to the computation of response functions of rigidly rotating waves in any other model of excitable tissue, as long as its right-hand sides are continuously differentiable so the linarized theory is applicable. Moreover, the method can also be extended in a straightforward way to include additional effects, such as the effect of uniform twist along scroll waves with linear filaments in three dimensions.

References

1. I. V. Biktasheva, D. Barkley, V. N. Biktashev, G. V. Bordyugov, A. J. Foulkes, Computation of the response functions of spiral waves in active media, Phys. Rev. E, **79**, to appear, (2009).
2. I. V. Biktasheva, Y. E. Elkin, and V. N. Biktashev, Localized sensitivity of spiral waves in the Complex Ginzburg-Landau Equation, Phys. Rev. E, **57**, 2656, (1998).
3. I. V. Biktasheva and V. N. Biktashev, Wave-particle dualism of spiral waves dynamics, Phys. Rev. E, **67**, 026221, (2003).
4. E. Hamm, Ph.D. thesis, Université de Nice - Sophia Antipolice / Institut Non Linéair de Nice, (1997).
5. H. Henry and V. Hakim, Scroll waves in isotropic excitable media: Linear instabilities, bifurcations, and restabilized states, Phys. Rev. E, **65**, 046235, (2002).
6. I. V. Biktasheva, A. V. Holden, and V. N. Biktashev, Localization of response functions of spiral waves in the FitzHugh-Nagumo system, IJBC, **16**, 1547, (2006).

2

Control of Spiral Wave Activity in Heterogeneous Excitable Media

Philip Bittihn[1], Eberhard Bodenschatz[1,3], Valentin Krinsky[1], Ulrich Parlitz[2], and Stefan Luther[1,3,4]

[1] Max-Planck-Institut für Dynamik und Selbstorganisation, Bunsenstraße 10, 37073 Göttingen, Germany
[2] Drittes Physikalisches Institut, Universität Göttingen, Friedrich-Hund-Platz 1, 37077 Göttingen, Germany
[3] Institut für Nichtlineare Dynamik, Universität Götttingen, Bunsenstraße 10, 37073 Göttingen, Germany
[4] Department of Biomedical Sciences, Cornell University, Ithaca, NY 14853, USA

Life-threatening cardiac arrhythmias are associated with the existence of stable and unstable spiral waves. Termination of such complex spatio-temporal patterns by local control is substantially limited by anchoring of spiral waves at natural heterogeneities. Far field pacing (FFP) is a new local control strategy that has been shown to be capable of unpinning waves from obstacles. Compared to a different local control strategy known as anti-tachycardia pacing (ATP), the superiority of FFP in unpinning spirals from obstacles (as an important step towards their removal) has been shown by numerical simulations in a previous study (Figures 3 and 5 in [2]).
In the present study, we investigate in detail the FFP unpinning mechanism in the Barkley model [1] for a single rotating wave pinned to a circular heterogeneity. We identify qualitatively different phase regimes of the rotating wave (Figure 2.1) showing that the concept of vulnerability is important but not sufficient to explain the failure of unpinning in all cases. Specifically, we find that a reduced excitation threshold can lead to the failure of unpinning even inside the vulnerable window, as defined in [4]. The critical value of the excitation threshold (below which no unpinning is possible) decreases for higher electric field strengths and larger obstacles. In some phase regimes, we also observe phase resetting of the spiral wave. This effect is important for the application of multiple stimuli in experiments.

We demonstrate that in the Barkley model the vanishing unpinning window effect is a fundamental limitation of FFP. A comparison with the well-known vulnerable window reveals that this is a genuinely two-dimensional effect. We find that spiral waves detach from the obstacle when the stimulus is inside the vulnerable window but that they can reattach after a short time if the stimulus is outside the unpinning window. The one-dimensional view that is generally taken cannot account for the interaction of the detached vortex with the refractory tail of the spiral wave. Not unexpectedly, in addition, we find that higher field strengths and bigger obstacles extend the range of excitability thresholds in which unpinning is possible and widen the unpinning window ρ_{uw}. The results are currently being published [3].

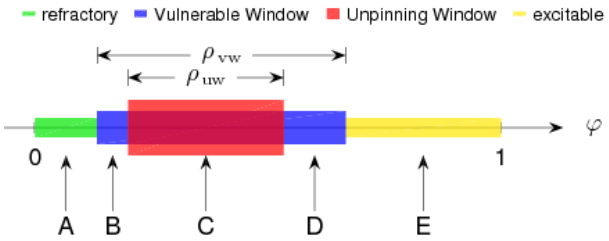

Fig. 2.1: Schematic structure of the unpinning window, viewed in the phase interval [0,1] (normalized position of the spiral on the circular obstacle boundary). The unpinning window ρ_{uw} is contained in the vulnerable window ρ_{vw} but does not necessarily span its whole width. **A**–**E** mark different FFP pulse times. **A** leads to no phase resetting, whereas **B**, **D** and **E** cause the phase to reset. **C** corresponds to successful unpinning.

References

1. Barkley, D., Kness, M., & Tuckerman, L. S. Spiral-wave dynamics in a simple model of excitable media: The transition from simple to compound rotation. *Phys. Rev.* A **42** 4, 2489 (1990).
2. Bittihn, Ph., Luther, G., Bodenschatz, E., Krinsky, V., Parlitz, U. & Luther, S. Far field pacing supersedes anti-tachycardia pacing in a generic model of excitable media. *New J. Phys.* **10**, 103012 (2008).
3. Bittihn, Ph., Squires, A., Luther, G., Bodenschatz, E., Krinsky, V., Parlitz, U. & Luther, S. Phase-Resolved Analysis of the Susceptibility of Pinned Spiral Waves to Far Field Pacing in a Two-Dimensional Model of Excitable Media, submitted to Philosophical Transactions of the Royal Society A
4. Starmer, C. F., Biktashev, V. N., Romashko., D. N., Stepanov, M. R., Makarova, O. N. & Krinsky, V. I. Vulnerability in an excitable medium: Analytical and numerical studies of initiating unidirectional propagation. *Biophys. J.* **65**, 1775 (1993).

3

Validation of effective medium theory for heterogeneous reaction-diffusion media

Sergio Alonso[1], Raymond Kapral[2], and Markus Bär[1]

[1] Physikalisch-Technische Bundesanstalt, Berlin, Germany
[2] Department of Chemistry, University of Toronto, Toronto, Canada

Fronts and pulses are typical travelling structures generated by reaction-diffusion processes. They are observed in chemical and biological media outside of equilibrium [1]. Reaction-diffusion systems can generate more complicated structures depending on the initial condition.

It is difficult to prevent heterogenities and deformations in experimental systems. These inhomogeneities modify the properties of such systems. It is also interesting to introduce artificial heterogeneities in a controlled fashion into the system to study their effects on wave propagation. Examples of heterogeneous reaction-diffusion sytems are the Belousov-Zhabotinsky reaction in oil microemulsions of water droplets [2] and the propagation of action potentials through cardiac tissue [3].

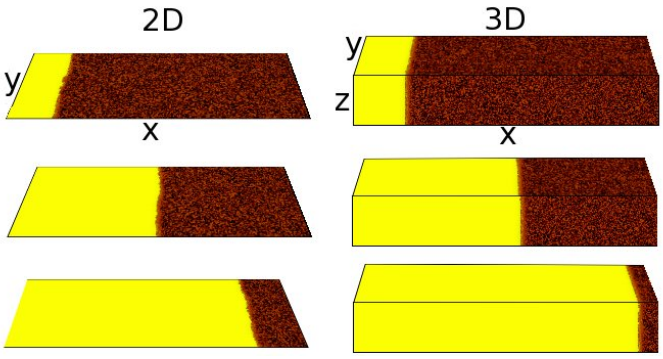

Fig. 3.1: Snapshots of bistable fronts (bright region) propagating from left to right in 2D (left column) and 3D (right column) heterogeneous media. Time evolution goes from top to bottom.

The small scale of the heterogeneities usually allows an effective description of the inhomogeneous system. Specific homogenization theories have been already suggested, but we propose a general effective medium theory based on the homogeneization of reaction-diffusion systems [4]. We consider a system where domains of phase 2 (heterogeneities) are randomly dispersed in a medium of phase 1. The reactivity and diffusion of the reactants take different values if they are inside or outside of such domains. If the heterogeneities are small, we can calculate effective values for the diffusion and the reactivity.

Here, we calculate the velocity of a front (see Fig 3.1) in a reaction-diffusion system under the presence of static obstacles. We obtain different results de-

pending on the type of the heterogeneities. We compare numerical results obtained with different types of obstacles with the predictions of the effective homogeneous medium theory [5].

The results can be applied to chemical and biological heterogeneous reaction-diffusion systems. We will finally discuss the applicability of the effective medium theory to dynamical evolution of the domains.

References

1. R. Kapral and K. Showalter (Eds.), *Chemical Waves and Patterns* (Kluwer, Dordrecht, 1994).
2. V. K. Vanag and I. R. Epstein, Phys. Rev. Lett. **87**, 228301 (2001).
3. A. V. Panfilov, Phys. Rev. Lett. **88**, 118101 (2002).
4. D. Bedeaux and R. Kapral, J. Chem. Phys. **79**, 1783 (1983).
5. S. Alonso, R. Kapral and M. Bär, Submitted (2009).

Control of spatio-temporal patterns in the Gray-Scott system

Y.N. Kyrychko[1], K.B. Blyuss[1], S.J. Hogan[1], and E. Schöll[2]

[1]Department of Engineering Mathematics, University of Bristol, Bristol, BS8 1TR, UK
[2] Institute für Theoretische Physik, TU Berlin, 10623 Berlin, Germany

In this talk I will present a systematic study of the effects of local time-delayed feedback control (TDFC) [1] on spatio-temporal dynamics in a two-component reaction-diffusion Gray-Scott model. It has already been shown using extensive numerical simulations that the Gray-Scott model supports a wide range of spatio-temporal dynamics, including stationary inhomogeneous patterns, travelling fronts and pulses, as well as spatio-temporal chaos. A particular feature of this system, which makes it different from other reaction-diffusion models, is the occurrence of pulse-splitting, where a travelling pulse leaves in its wake other pulses propagating in different directions.

The Gray-Scott system can be written as [2]

$$\begin{aligned} \frac{\partial u}{\partial t} &= -uv^2 + a(1-u) + D_u\nabla^2 u = f(u,v) + D_u\nabla^2 u, \\ \frac{\partial v}{\partial t} &= uv^2 - (a+b)v + D_v\nabla^2 v = g(u,v) + D_v\nabla^2 v, \end{aligned} \tag{4.1}$$

where u and v are the concentrations of the species U and V, respectively, a is the inflow rate, $a+b$ is the removal rate of V from the reaction, and D_u and D_v are the diffusion coefficients of the two species.

Formally, the locally controlled Gray-Scott model can be written as

$$\frac{\partial}{\partial t}\begin{pmatrix} u \\ v \end{pmatrix} = \begin{pmatrix} f(u,v) \\ g(u,v) \end{pmatrix} + \begin{pmatrix} D_u & 0 \\ 0 & D_v \end{pmatrix}\nabla^2 \begin{pmatrix} u \\ v \end{pmatrix} + KA\begin{pmatrix} u(t-\tau)-u(t) \\ v(t-\tau)-v(t) \end{pmatrix},$$

where K is the control strength which can be either positive or negative, $\tau > 0$ is the time delay.

The results of the numerical simulations of the Gray-Scott model (4.1) using the TDFC are presented in the Figures 4.1 and 4.2. They show that local TDFC can provide a variety of interesting dynamical regimes, from stationary patterns to mixed modes and travelling localized pulses. Numerical simulations suggest that in many cases the control strength does not have to be very high, provided time-delay is large enough.

References

1. K. Pyragas, Continuous control of chaos by self-controlling feedback, Phys. Lett. A 170 (1992) 421-428.
2. P. Gray and S.K. Scott, Autocatalytic reactions in the isothermal, continuous stirred tank reactor: Oscillations and instabilities in the system $A + 2B \to 3B$, $B \to C$, Chem. Engng. Sci. 39 (1984) 1087-1097.

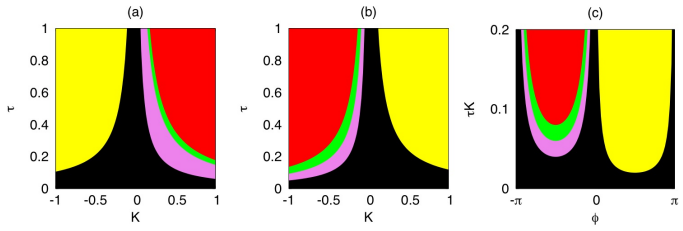

Fig. 4.1: Control domain of spatio-temporal chaos. (a) Activator control. (b) Inhibitor control. (c) Phase diagram for non-diagonal control. Colour denotes a specific final state: spatio-temporal chaos (black), stable mixed (Turing-Hopf) state (pink), coarsening (green), bi-stability between travelling waves and a trivial steady state (red) and a uniform non-trivial steady state (yellow). Parameter values are $a = 0.028$, $b = 0.053$, $D_u = 2 \cdot 10^{-5}$, $D_v = 10^{-5}$.

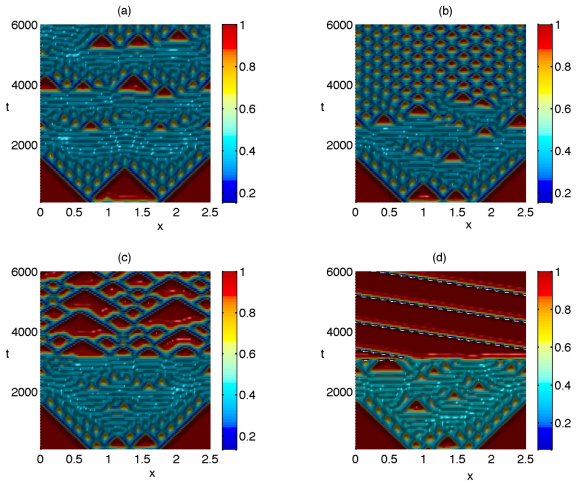

Fig. 4.2: Space-time plot in the case of inhibitor control. (a) Spatio-temporal chaos. (b) Mixed (Turing-Hopf) mode. (c) Coarsening. (d) Transition to travelling waves. Parameter values are $a = 0.028$, $b = 0.053$, $D_u = 2{\cdot}10^{-5}$, $D_v = 10^{-5}$, (a) $K = -0.05$, $\tau = 0.3$, (b) $K = -0.3$, $\tau = 0.35$, (c) $K = -0.4$, $\tau = 0.4$ and (d) $K = -0.6$, $\tau = 0.75$. Control is switched on at $t = 3000$.

5

Statistical Analysis of Heteroclinic Turbulence in Diffusion Lotka-Volterra Equation

Kenji Orihashi and Yoji Aizawa

Department of Applied Physics, Waseda University, Tokyo, Japan
e-mail: orihashi-1026@aoni.waseda.jp

In mathematical biology, the diffusion Lotka-Volterra equation has been studied to analyze population dynamics, and many studies have been performed [1]- [8]. In particular, the traveling wave [6,7] and the spatio-temporal chaos [8] are studied. So the behavior of the equation has attracted many attention. A heteroclinic cycle is a topological circle connecting several equilibrium points in phase space. And in some case, a turbulence is generated by the interaction between the heteroclinic cycle and the diffusion effect, for instance, the Lotka-Volterra system [8] ,the replicator equation [9] and the Gray-Scott model [10].

Let us consider the following competitive Lotka-Volterra reaction diffusion equation:

$$\begin{cases} \dfrac{\partial Y_1}{\partial t} = Y_1(1 - Y_1 - \alpha Y_2 - \beta Y_3) + \dfrac{\partial^2 Y_1}{\partial r^2}, \\ \dfrac{\partial Y_2}{\partial t} = Y_2(1 - \beta Y_1 - Y_2 - \alpha Y_3) + \dfrac{\partial^2 Y_2}{\partial r^2}, \\ \dfrac{\partial Y_3}{\partial t} = Y_3(1 - \alpha Y_1 - \beta Y_2 - Y_3) + \dfrac{\partial^2 Y_3}{\partial r^2}, \\ (0 \le Y_i(r,t), \quad [0 \le r \le L]) \end{cases} \tag{5.1}$$

where $Y_i = Y_i(r,t)$ is the population of the ith species ($i = 1,2,3$), α and β are positive parameters, and L is the system size. We assume the spacial dimension to be unity and the boundary condition to be periodic, and the interaction matrix is a cyclic one (May-Leonard type). α, β, and L are bifurcation parameters of Eq. (5.1).

First, the bifurcation diagrams of (α, β) for several L are demonstrated in detail, and it is emphasized that the diversity of the attractor enhances when the system size increases. When L is small, only two spatially uniform solutions exist. When L is large, not only two spatially uniform solutions but also turbulence and traveling wave are observed. Next, the transition from a regular attractor to a turbulent one is characterized by correlation length and time, as well as by Lyapunov exponent and Lyapunov dimension. For these characteristics, the scaling relations are observed. And comparing to the case of diffusion replicator equation [9], the similarity points and the different points between the two equations are reported. Finally, the onset mechanism of the turbulence are theoretically discussed by using the phase reduction method.

References

1. L. J. S. Allen, Math. Biosci. **65**, 1 (1983).

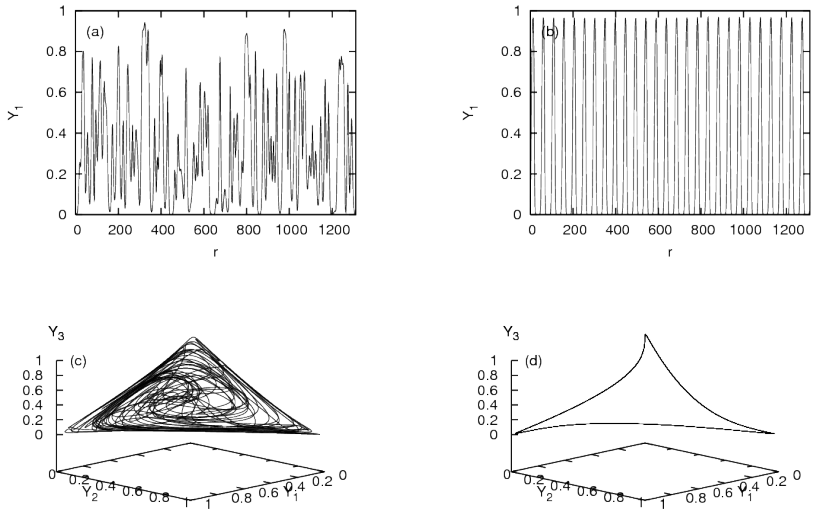

Fig. 5.1: Snap shots of $Y_1(r,t)$; (a) for the turbulence ($\alpha = 0.1$, $\beta = 2.6$), and (b) for the traveling wave ($\alpha = 0.1$, $\beta = 5.8$). Three-dim. embedding plots of those snap shots are shown (c) and (d).

2. C. Cosner and A. C. Lazer, SIAM J. Appl. Math. **44**, 1112 (1984).
3. E. E. Holmes, M. A. Lewis, et al., Ecology, **75**, 17 (1994)
4. S. A. Gourley and N. F. Britton, J. Math. Biol. **34**, 297 (1996).
5. G. Gambino, M. C. Lombardo and M. Sammartino, Appl. Num. Math. **59**, 1059 (2009).
6. L. Zhang, L. F. Zhang, et al., ACTA Physica sinica **58** 703 (2009).
7. C. V. Pao, J. Math. Anal. Appl. **281**, 186 (2003).
8. S. V. Petrovskii, B. L. Li, and H. Malchow, Bull. Math. Biol. **65**, 425 (2003).
9. K. Orihashi and Y. Aizawa, Physica D 237, 3053 (2008)
10. Y. Nishiura and D. Ueyama, Physica D 150, 137 (2001)

6

On data assimilation through variational calculus

J. Bröcker and I. G. Szendro Terán

Max-Planck Institut für Physik komplexer Systeme
Nöthnitzer Strasse 38
01187 Dresden
Germany

Time series are often assumed to arise as observations from an underlying dynamical system. The observations though need not be one–to–one mappings of the full state of the underlying dynamical system, which is thus only partially observed. Both for the purpose of analyzing such systems as well as forecasting future observations, it is usually necessary to compute trajectories which are on the one hand consistent with some proposed model of the dynamics, but which on the other hand closely follow (or 'shadow') the recent history of observations. This process (referred to as data assimilation in the atmospheric sciences or smoothing in the engineering community) is revisited in this contribution. As currently employed (for example in weather forecasting), variational methods meet with the fundamental difficulty that the corresponding normal equations are ill–posed. For this reason, only very short observation windows can be taken into account. In this contribution, an approach to data assimilation using concepts from nonlinear control theory will be presented. The model dynamics are augmented by a control force, which is chosen so as to make the discrepancy between the trajectory and the actual observations, the tracking error, small. At the same time, large control actions are penalized as well, in order to create trajectories which are as consistent with the (uncontrolled) model dynamics as possible. Provided there is no model error, the control is expected to vanish once the dynamics is "on track". In the presence of model error though, a small but non-vanishing control will remain necessary to keep the trajectory close to the observations. It is demonstrated that this approach provides an effective means to regularize the problem, and to control the trade-off between perfectly following the observations and perfectly obeying the model dynamics. Furthermore, an ex–post analysis of the control forces should provide information on model imperfections.

7

Pattern formation and chaotic dynamics in a cross-flow catalytic TWC reactors

M. Kohout[1], O. Hadač[1], J. Havlica[2], and I. Schreiber[1]

[1] Department of Chemical Engineering, Center for Nonlinear Dynamics of Chemical and Biological Systems, Institute of Chemical Technology, Prague, Technická 5, 166 28 Prague 6, Czech Republic, email: Martin.Kohout@vscht.cz
[2] Institute of Chemical Process Fundamentals, Academy of Sciences of the Czech Republic, Rozvojová 135, 165 02 Prague 6, Czech Republic

Dynamics of models describing catalytic oxidation of CO and C_2H_2 and reduction of NO_x taking place in a cross-flow tubular reactor are examined.

We begin with a detailed kinetic model proposed for three-way catalytic converters. In an effort to relate resulting patterns to specific pathways in the mechanism we select two reaction subsystems combining CO oxidation with oxidation of C_2H_2 and with NO_x reduction. The ability of these two subsystems to generate nonlinear dynamical effects is examined first by neglecting transport phenomena and studying a lumped (CSTR) system with the use of stoichiometric network and bifurcation analysis.

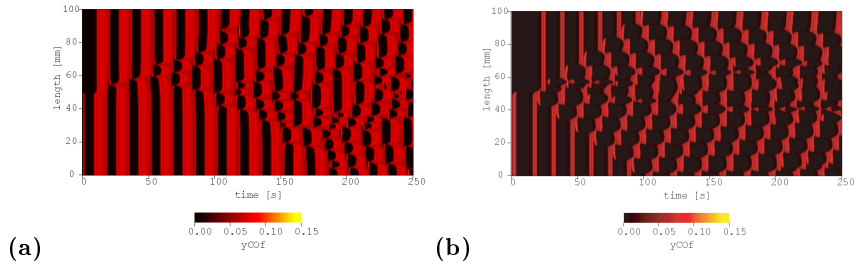

Fig. 7.1: The space-time plot of spatiotemporal chaotic pattern in reaction–diffusion convection system in a TWC; the inlet oxygen concentration (a) – $y^{\mathrm{in}}_{\mathrm{O}_2} = 0.535$ mol. % and the temperature $T^{\mathrm{in}} = 490.0$ K, (b) – $y^{\mathrm{in}}_{\mathrm{O}_2} = 0.50$ mol. % and $T^{\mathrm{in}} = 496.0$ K.

Spatiotemporal behavior due to reaction kinetics combined with transport processes have been further studied in tubular reactor with cross-flow (TFR). Based on knowledge of the lumped dynamics, the observed spatiotemporal patterns are classified as phase waves, travelling front and pulse waves and chaotic spatiotemporal patterns (see Fig. 7.1). Their dependence on input parameters are systematically studied and their relation to different unstable reaction pathways is discussed.

8

Pattern dynamics in thin free-standing smectic films

K. Harth, C. Bohley, A. Eremin, and R. Stannarius

Otto von Guericke University Magdeburg, Institute of Experimental Physics

Free-standing films of thermotropic smectic tilted phases (smC, smC*) represent the simplest quasi two-dimensional anisotropic liquids. Distortions of the local tilt-azimuth orientation of the mesogens (**c**-director) generate elastic forces and torques. By studying director structures in external electric fields and their free relaxation from non-equilibrium states of the elastic energy one can explore the coupling between orientation and flow fields in the films. Such coupling effects represent unique features of anisotropic liquids.

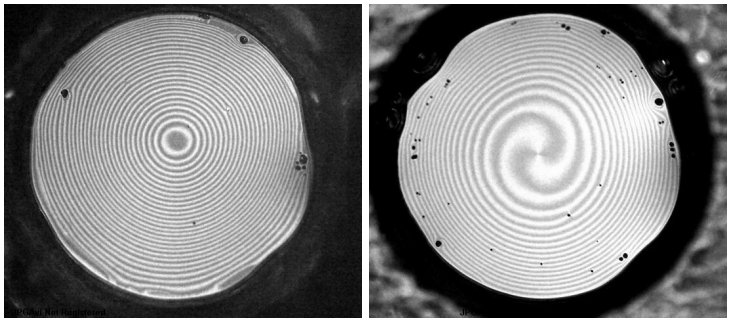

Fig. 8.1: Target(left) and spiral (right) pattern of a freely suspended smectic C* film (the film width is 3 mm) under slightly decrossed polarizers. The dark dots are tracer particles for the visualisation of the flow fields.

Experiments are performed with a polarised light microscope. We prepare simple director states by means of external electric fields, for example those appearing as targets or spirals (Fig. 8.1), and study the temporal texture evolution. The dynamics of the **c**-director is extracted from these textures. Simultaneously, we visualise the in-plane flow with small probe particles. It is demonstrated that macroscopic flow patterns can be generated by inhomogeneous director relaxation.

The dynamic equations - incompressible anisotropic Navier-Stokes equation and torque balance equation - are solved numerically with standard finite element methods (COMSOL). The calculated flow fields and director relaxation characteristics are utilised to extract information on the five involved viscosities and two elastic constants of the liquid crystalline material.

Experiments with films that contain inclusions (droplets or solid particles) widen the opportunities to access elastic properties and allow to observe a variety of pattern forming phenomena. In addition to the standard splay and bend elastic constants, a spontaneous bend elastic term is allowed by

symmetry in chiral phases. Even though the involved free energy term can be transformed into a surface integral by the Stokes integral theorem, so that the bulk equations are not influenced by it, we can demonstrate a geometry where the spontaneous bend takes effect: The director field around inclusions with rigid anchoring depends upon the spontaneous bend (Fig. 8.2). The observed textures allow to determine the respective elastic constant quantitatively.

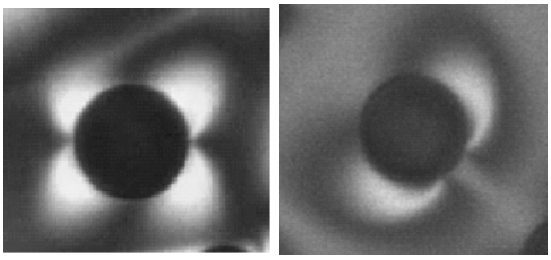

Fig. 8.2: Isotropic liquid droplet in a freely suspended film. The **c**-director is anchored tangentially at the film boundaries, two defects of strength 1/2 appear at the droplet boundaries. Their arrangement can be symmetrical on opposite sides of the droplet, so-called quadrupolar configuration (left image), or shifted towards one side of the droplet by the effect of the spontaneous bend term, so-called dipolar configuration (right image).

Inclusions in free-standing smectic films can be considered as very simple and conveniently handled model systems for two-dimensional colloids. We discuss several topological interactions mediated by the director field and self-organisation of inclusions into chains and lattices [2].

References

1. P. V. Dolganov and V. K. Dolganov, *Phys. Rev. E*, **73** 041706, (2006)
2. C. Bohley and R. Stannarius. *Soft Matter*, **4** 683, (2008).

9

Stoichiometric network analysis in chemical reaction mechanisms

O. Hadač, M. Kohout, I. Schreiber, V. Nevoral, and M. Marek

Department of Chemical Engineering, Center for Nonlinear Dynamics of Chemical and Biological Systems, Institute of Chemical Technology, Prague, Technická 5, 166 28 Prague 6, Czech Republic, Otto.Hadac@vscht.cz

The stoichiometric networks analysis [1,2] provides a natural way of decomposing the entire chemical network into elemental subnetworks. This methodology also identifies those among them that are possible sources of complex dynamical behaviour [3]. Identification of the unique set of systematically independent subnetworks (reaction pathways or currents) called extreme pathways/currents is the main goal of this contribution. In geometrical terms, the extreme currents represent the edges of the steady-state flux cone. The steady-state flux cone is the space of all admissible (i.e. non-negative) rate vectors that is the affine linear subspace. A polynomial differential system describes the behaviour of a chemical network with generalized mass action kinetics. This sparse polynomial system is defined by a weighted directed graph and a weighted bipartite graph [4]. In this application, the number of real positive solutions within certain affine subspaces is of particular interest. In general, the positive steady states of chemical reaction systems are strongly determined by the properties of the two graphs. In the stoichiometric network analysis the set of steady-state solutions is considered as a convex polyhedral cone. We use an efficient algorithm that determines the set of extreme currents suitable for both homogeneous and heterogeneous catalytic systems. The algorithm [5] is pathway-oriented due to the reduction of combinatorial possibilities of choice of the reactions.

References

1. B.L. Clarke, Stability of complex reaction networks, Adv. Chem. Phys. **43**, 1 (1980).
2. J. Ross, I. Schreiber, & M.O. Vlad, Determination of complex reaction mechanisms, Oxford University Press, New York 2006.
3. M. Marek, M. Schejbal, P. Kočí, V. Nevoral, M. Kubíček, O. Hadač, & I. Schreiber, Oscillations, period doublings, and chaos in CO oxidation and catalytic mufflers, Chaos **16**, 037107 (2006).
4. K. Gatermann, B. Hubber, A family of sparse polynomial systems arising in chemical reaction systems, J. Symbolic Computation **33**, 275 (2002).
5. C.H. Schilling, D. Letscher, B.Ø. Palsson, Theory for the systemic definition of metabolic pathways and their use in interpreting metabolic function from a pathway-oriented perspective, J. Theor. Biol. **203**, 229 (2000).